letters

Carboxyl proteinase from *Pseudomonas* defines a novel family of subtilisin-like enzymes

Alexander Wlodawer[1], Mi Li[1,2], Zbigniew Dauter[3], Alla Gustchina[1], Kenichi Uchida[4], Hiroshi Oyama[5], Ben M. Dunn[6] and Kohei Oda[5]

[1]*Protein Structure Section, Macromolecular Crystallography Laboratory, National Cancer Institute at Frederick, Frederick, Maryland 21702, USA.* [2]*Intramural Research Support Program, SAIC Frederick, National Cancer Institute at Frederick, Frederick, Maryland 21702, USA.* [3]*Synchrotron Radiation Research Section, Macromolecular Crystallography Laboratory, National Cancer Institute and NSLS, Brookhaven National Laboratory, Bldg. 725A-X9, Upton, New York 11973, USA.* [4]*Department of Biosciences, School of Science and Engineering, Teikyo University, 1-1 Toyosatodai, Utsunomiya 320-8551, Japan.* [5]*Department of Applied Biology, Faculty of Textile Science, Kyoto Institute of Technology, Sakyo-ku, Kyoto 606-8585, Japan.* [6]*Department of Biochemistry and Molecular Biology, University of Florida, Gainesville, Florida 32610, USA.*

The crystal structure of a pepstatin-insensitive carboxyl proteinase from *Pseudomonas* sp. 101 (PSCP) has been solved by single-wavelength anomalous diffraction using the absorption peak of bromide anions. Structures of the uninhibited enzyme and of complexes with an inhibitor that was either covalently or noncovalently bound were refined at 1.0–1.4 Å resolution. The structure of PSCP comprises a single compact domain with a diameter of ~55 Å, consisting of a seven-stranded parallel β-sheet flanked on both sides by a number of helices. The fold of PSCP is a superset of the subtilisin fold, and the covalently bound inhibitor is linked to the enzyme through a serine residue. Thus, the structure of PSCP defines a novel family of serine-carboxyl proteinases (defined as MEROPS S53) with a unique catalytic triad consisting of Glu 80, Asp 84 and Ser 287.

The pepstatin-insensitive carboxyl proteinase (PSCP) from *Pseudomonas* sp. 101 has been studied for almost 15 years[1–4]. PSCP is a homolog of CLN2, a human enzyme associated with a serious neurodegenerative disease (see below). Although a number of aspartic acid and glutamic acid residues have been implicated in the catalytic activity of PSCP[3,4], its lack of sequence similarity to known aspartic proteinases[5,6] indicates that it is not a typical member of this family. In addition, no extensive sequence similarity between PSCP and other proteolytic enzymes of known structure has been detected; therefore, its fold has not yet been predicted.

Comparisons of the primary structures of PSCP with seven other similar enzymes revealed that they can be categorized as members of a unique family (17.5–50% sequence identity). The other related bacterial enzymes include *Xanthomonas* sp. T-22 carboxyl proteinase (XCP)[1]; kumamolysin (KCP), an enzyme isolated from the thermophilic bacterium *Bacillus* novosp. MN-32 (ref. 7); and alcohol-resistant proteinase J-4, isolated from the bacterium *Bacillus coagulans*[8]. Another important member of this class of proteinases is CLN2, a human enzyme that leads to the fatal neurodegenerative disease, classical late-infantile neuronal ceroid lipofuscinosis[9], when mutated. CLN2 was recently identified as a tripeptidyl-peptidase I and predicted to be a serine proteinase[10,11]. Two other enzymes related to PSCP are the recently identified putative serine proteinases Lys60 and Lys45, markers for late lysosomes in *Amoeba proteus*[12]. No natural substrates for any of the enzymes discussed above have been identified.

We show here that the *Pseudomonas* enzyme PSCP can be described, based on its three-dimensional structure, as a defining member of a new family of serine proteinases. We propose to name this family serine-carboxyl proteinases, with the *Pseudomonas* enzyme being abbreviated PSCP (*Pseudomonas* serine-carboxyl proteinase), rather the previous abbreviation PCP[3]. This new family has now been classified as S53 in the MEROPS database[6].

Description of the structure of PSCP

The fold of PSCP (Fig. 1) is based on a seven-stranded all-parallel β-sheet consisting of strands s2–s3–s1–s4–s5–s6–s7b. The sheet is flanked on one side by helices h4 and h5 and on the other by h2′, h3, h6 and h8 (Fig. 2). These helices are parallel to each other but antiparallel to the strands in the β-sheet. All of these helices except for h2 are also involved in creating the extensive hydrophobic core of the molecule. Two helices, h6 and h3, are buried in the central part of the molecule, with the surface helix h2′ interacting with h3. Although the helices on the other side of the sheet, h4 and h5, provide an extensive buried surface, they are partially exposed to the surface of the protein. The second and third β-strand, s2 and s3, located at the edge of the central sheet are connected by helix h3 in a rare left-handed crossover that was first described for subtilisin[13]. The fold of the protein is completed by several other shorter strands and helices, with three pairs of strands (s8–s9, s6′b–s6″a and s6″b–s7a) forming β-hairpins on the surface of the protein (Fig. 2).

Two proline residues, Pro 192 and Pro 260, are found in *cis* conformation. Pro 192, which is located in a stretch of irregular
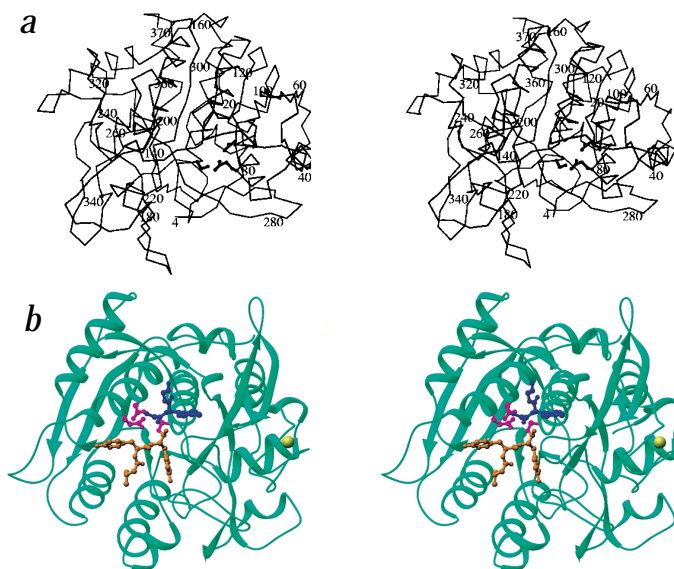

a

b

Fig. 1 Two views of the PSCP molecule. *a*, Stereo tracing of the Cα backbone of PSCP (crystal D), with the side chains of the putative active site residues (Ser 287, Glu 80, Asp 84) in ball-and-stick representation. Every 20th residue is labeled. Figure prepared with Molscript[34]. *b*, Ribbon diagram showing protein in green, active site residues in pink, Ca2+ ion in yellow, and the inhibitor found in crystals B and C in gold and blue, respectively. Figure prepared using Ribbons[35].
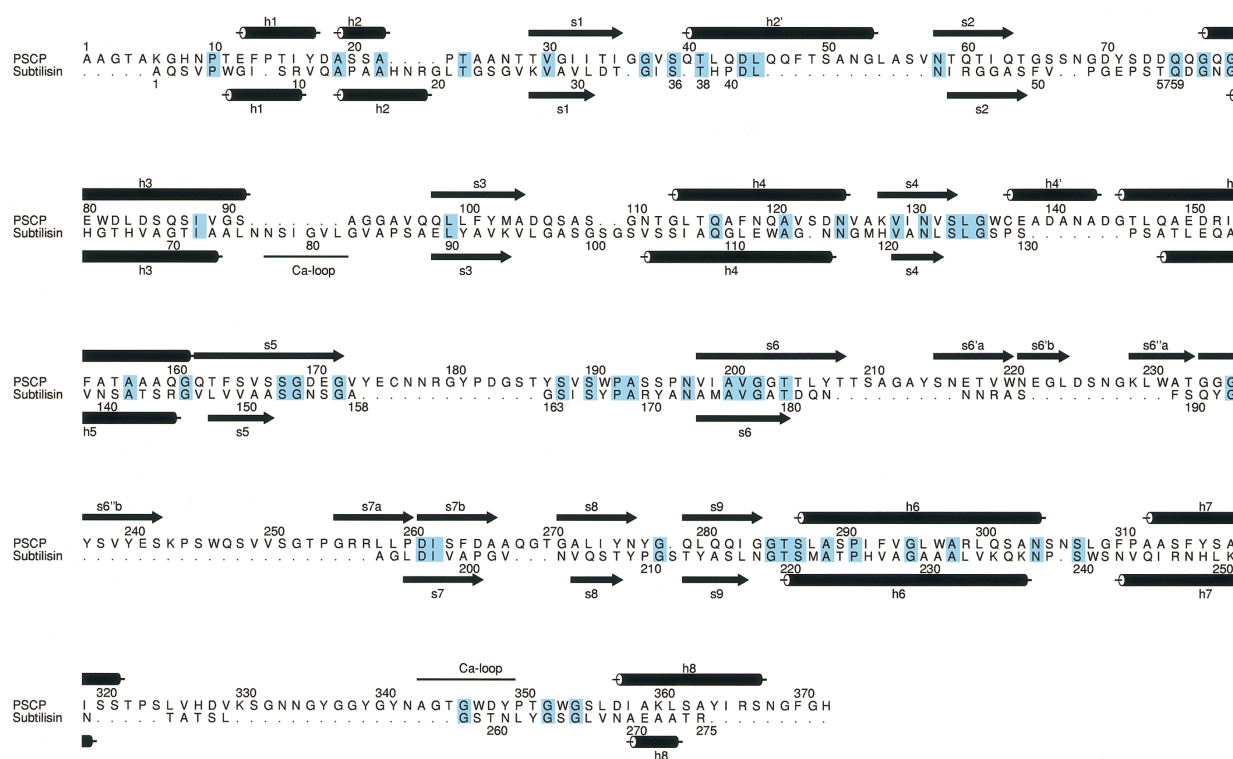
Fig. 2 Structure-based sequence alignment of PSCP and subtilisin (PDB code 1GCI)[15]. Identical residues are highlighted in blue and the secondary structure elements are marked above and below the sequence of each enzyme. Every major secondary structure element identified in the structure of subtilisin has a counterpart in PSCP, although the latter is significantly larger and has a number of additional secondary structure elements. For this reason, we introduce a convention for naming the secondary structure elements in PSCP that uses identical designations for the strands and helices found in both enzyme families, with prime symbols for elements present only in PSCP and letters 'a' and 'b' for those significantly longer in PSCP. Strands are split as necessary, based on their interaction partners. This fold similarity does not extend to the conservation of the residues, because the level of identity between structure-aligned sequences is rather low. We identified 54 residues common to subtilisin and PSCP, representing ~20% of the sequence of the former and only 14.5% of the latter. Nevertheless, some of the identical residues are located in areas crucial to the preservation of the fold, with 14 being either glycine or proline, including the *cis* Pro 192 in PSCP (corresponding to *cis* Pro 168 in subtilisin).
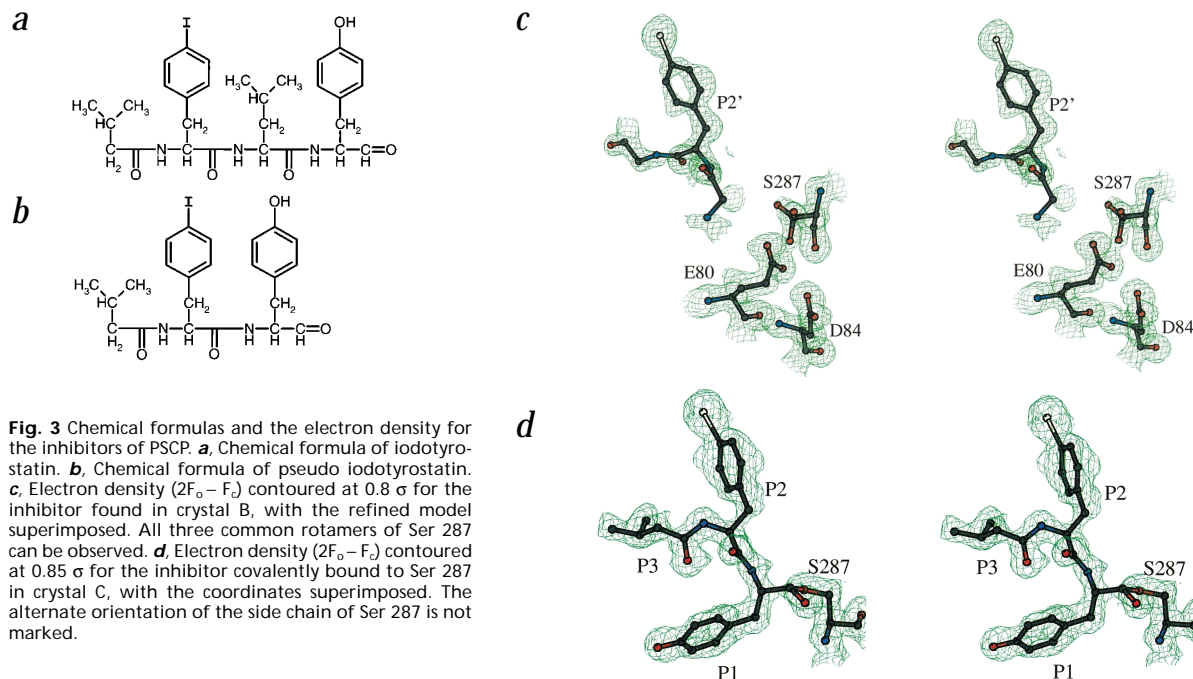

Fig. 3 Chemical formulas and the electron density for the inhibitors of PSCP. *a*, Chemical formula of iodotyrostatin. *b*, Chemical formula of pseudo iodotyrostatin. *c*, Electron density ($2F_o - F_c$) contoured at 0.8 σ for the inhibitor found in crystal B, with the refined model superimposed. All three common rotamers of Ser 287 can be observed. *d*, Electron density ($2F_o - F_c$) contoured at 0.85 σ for the inhibitor covalently bound to Ser 287 in crystal C, with the coordinates superimposed. The alternate orientation of the side chain of Ser 287 is not marked.
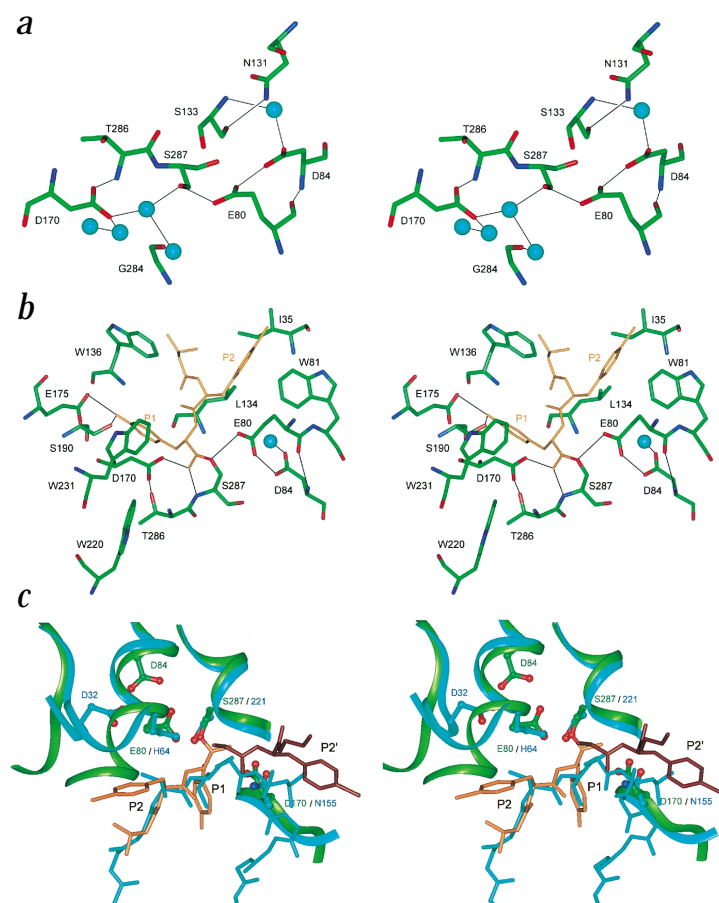
letters

Fig. 4 Residues forming the active site of PSCP in comparison with subtilisin. *a*, Residues in the active site of the uninhibited crystal D and the network of hydrogen bonds involving these residues and adjacent water molecules (see text for discussion). For simplicity, only the principal orientation of Ser 287 is shown. Hydrogen bonds are marked in thin black lines. *b*, The inhibitor pseudo iodotyrostatin bound in the active site of crystal C (gold), together with selected residues of PSCP. Only the principal orientations of the residues are shown, and hydrogen bonds are marked in thin black lines. *c*, Comparison of the substrate-binding areas of PSCP (green) and subtilisin (blue), the latter complexed with eglin C[22]. Both the inhibitors seen in crystals B (orange) and C (brown) are aligned with eglin C (blue).

of subtilisin, Ser 287 in PSCP is equivalent to Ser 221 in subtilisin both in the primary and tertiary structures (Figs 1, 2) and is an obvious candidate for the primary catalytic residue in the active site.

Glu 80 can form a hydrogen bond with Ser 287 and can interact, through its side chain, with Asp 84 (Fig. 4*a*). The close distance between the carboxylates of Glu 80 and Asp 84 (~2.6 Å) indicates that a proton is shared between these residues in all the structures because the electrostatic repulsion of charged groups would prevent their close contact. Both Glu 80 and Asp 84 originate from helix h3, a structural element involved in creating a left-handed crossover that is usually found in protein areas important for activity[17]. Although Glu 80 is a structural equivalent of His 64 in subtilisin, Asp 84 is not structurally related to Asp 32 in subtilisin, the third member of the catalytic triad[18]. Presumably, the active sites of these enzymes resulted from separate evolutionary events.

At least one other residue can be defined as crucial to the catalytic activity of PSCP; this residue is Asp 170, which in subtilisin is structurally equivalent to Asn 155 (Fig. 4*c*). In subtilisin, the side chain of Asn 155 creates part of the oxyanion hole stabilizing the tetrahedral intermediate of the reaction. The orientation of the side chain of Asp 170 is the same in all PSCP structures. In the native enzyme, the orientation is maintained by the interactions with Ser 287 through a water molecule. That water is replaced by a hydroxyl when the inhibitor covalently binds to Ser 287 (Fig. 4*a,b*).

The roles of various side chains in the binding and catalytic activities of PSCP and XCP have been investigated by site-directed mutagenesis. Oyama *et al.*[4] mutated eight conserved Glu or Asp residues in both PSCP and XCP to Ala. Asp 84, 170 and 328 in PSCP (or their equivalents in XCP) were found to be essential either to the self-activation of the proenzyme form or to the cleavage of peptide substrates[4]. In particular, replacement of Asp 84 led to a 10[4]-fold decrease in catalytic activity in PSCP. The structure reported here confirms that Asp 84 and Asp 170 are critical catalytic residues, whereas Asp 328 is involved in creating a Ca^{2+}-binding site, an important structural element of the protein. No mutation data for Glu 80 or its equivalent in other enzymes are available at this time. The putative nucleophilic Ser 287 residue has been replaced by Ala in XCP and KCP with complete loss of catalytic activity (H. Oyama and K. Oda, unpublished).

structure located between strands s5 and s6, sharply changes the direction of the peptide chain. Pro 260 creates a kink between strands s7a and s7b. Both of these *cis* prolines appear to be required because of steric constraints of the local structure. The sole disulfide bridge in PSCP connects Cys 137 and Cys 176. A prominent octahedrally-coordinated Ca^{2+}-binding site is liganded by two carboxylate oxygens of Asp 328 and Asp 348, three amide carbonyl groups of residues 329, 344 and 346, and a clearly defined water molecule.

A structural similarity search, performed with the program DALI[14], unambiguously identified this enzyme as a new member of the subtilisin clan (SB) of serine proteinases[6]. The Z-score between PSCP and the highest-resolution structure of subtilisin[15] was 24.4, with the root mean square (r.m.s.) deviation of 2.5 Å between 238 Cα pairs. Thus, the fold of PSCP can be described as a superset of the subtilisin fold[16], in which this substantially larger enzyme (372 amino acids *versus* ~275 for subtilisin) is folded with an identical overall topology. However, PSCP contains a number of extra secondary structure elements inserted into loops corresponding to those connecting the strands and helices in subtilisin (Fig. 2).

The active site of PSCP

The active site of PSCP can be identified based on the binding of a covalent inhibitor. A complete molecule of the inhibitor pseudo tyrostatin bound to Ser 287 (Fig. 3*b*; also see the next section) could be traced in one of the crystals (Table 1). The aldehyde of the inhibitor makes an unambiguous hemiacetal linkage to the OG of Ser 287 (Figs 3*d*, 4*b*). Because the fold of PSCP corresponds to that

Interactions between the inhibitors and the enzyme

The inhibitor covalently attached to PSCP in one of the crystals was identified as pseudo iodotyrostatin (Figs 3*b*, 4*b*; see Methods). The C-terminus of the inhibitor and the OG oxygen of Ser 287 covalently bond to form a hemiacetal, with the carbon

atom bound to the serine with *S* chirality. Analogous linkages have been described for the complexes of chymostatin, a related inhibitor, and two serine proteinases, *Streptomyces griseus* proteinase A[19] and wheat serine carboxypeptidase II (ref. 20). Both stereoisomers of the hemiacetal linkage were reported for the structure of proteinase A, whereas only *R* stereochemistry was reported for carboxypeptidase. Thus, the chirality of the active site of PSCP is opposite to that of carboxypeptidase, which agrees with the oberservation of Bullock *et al.*[20], who noted that the arrangement of the active site residues in carboxypeptidase corresponds to a mirror image of the arrangement in subtilisin.

The three visible side chains of pseudo iodotyrostatin define subsites S3–S1 of the substrate binding site[21]. The side chain of P1 Tyr is wedged into a pocket created by the side chain of Arg 179, the main chain of residues 133–136 and the main and side chains of residues 167–170 (Fig. 4*b*; some residues not shown for clarity). The OH atom of P1 Tyr makes a hydrogen bond with OE2 of Glu 175; thus, this pocket seems to be ideally suited for accommodating a tyrosine. The location of this side chain is almost identical to that of the P1 ligand side chains in several inhibitor and substrate complexes of subtilisin (Fig. 4*c*). This reinforces our interpretation that the mode of binding of pseudo iodotyrostatin observed at low pH is relevant to the mode of binding of a substrate of PSCP. The iodoPhe residue of pseudo iodotyrostatin occupies a rather open area bound on one side by the side chains of Ile 35, Asp 74, Trp 81 and Glu 80, while exposed to the solvent on the other side. The iodine atom interacts with the carboxylate of Asp 74 (not shown). The amide bond between the P1 and P2 residues is almost completely superimposable with the corresponding amide in a complex of subtilisin with eglin C[22], with the Cα and Cβ atoms of the side chain in almost identical positions (Fig. 4*c*).

Although the N-terminal isovaleryl group of the inhibitor has well-defined electron density, it does not make any clear contacts with the enzyme. The sole interaction orienting this residue is a hydrogen bond between the carbonyl of its main chain peptide and the amide nitrogen of residue 135. This particular interaction is also completely superimposable on the structurally equivalent part of eglin C complexed to subtilisin, although the side chain of the isovaleryl group points along the main chain of eglin C in the subtilisin complex and may not really point into the true subsite S3. Nevertheless, the agreement between the mode of binding of pseudo iodotyrostatin and the ligands of subtilisin indicates that at least the S1 and S2 pockets are formed in PSCP and subtilisin in a similar fashion.

Fragments of the inhibitor are also seen in an orientation different from the one described above in one of the high pH crystals. There is no indication of any covalent bond between the inhibitor and Ser 287; the visible portion of the inhibitor, consisting of the iodoPhe residue and the main chain atoms of the adjacent residues (modeled as glycines), occupy parts of the S1′–S3′ pockets. This interpretation is again supported by comparisons with the structure of the subtilisin–eglin C complex,

because the position of P2′ iodoPhe corresponds well to the P2′ residue in eglin C (Fig. 4*c*), even though the chain is shifted by almost 2 Å while maintaining similar torsion angles. The side chain of the P2′ residue makes excellent parallel stacking interactions with the indole ring of Trp 231 and perpendicular interactions with Trp 220 (data not shown). These two residues originate from a region of PSCP that has no equivalent in subtilisin; therefore, the difference between the exact locations of the active site pockets that would bind the C-terminus of the peptide to be cleaved is not surprising. The area corresponding to the S3′ site in PSCP is different from its counterpart in subtilisin.

The mode of enzymatic activity

It has been established that enzymes in the PSCP family are active in the pH range of 3–5 (ref. 23), leading to early hypotheses that these were aspartic proteinases. Although determining the detailed mechanism of action of PSCP will require additional experimental and computational data, some preliminary analysis based on the available structures is possible. As the side chain oxygen atom of Ser 287 approaches the carbonyl carbon of

Table 1 Details of X-ray data collection and refinement

Crystal	A	B	C	D
Description	NaBr peak	Inhibitor at P′ site	Covalent inhibitor	Native
Data collection				
pH	7.5	7.5	4.0	5.2
Unit cell dimensions (Å) of space group P6$_2$				
a = b	97.3	97.19	97.63	97.40
c	83.0	83.37	83.30	83.35
Wavelength (Å)	0.9191	0.92	0.98	0.98
Resolution (Å)	1.8	1.4	1.4	1.0
Measured reflections	228,827	677,827	529,714	2,554,920
Unique reflections	41,335	87,947	88,568	241,182
R_{merge} (%)[1]	4.1 (32.7)	3.6 (21.6)	7.4 (66.0)	5.4 (47.7)
R_{anom} (%)[1]	4.1 (19.3)	–	–	–
I/σ(I)[1]	23.4 (3.2)	50.2 (7.0)	23.3 (2.3)	38.7 (4.7)
Completeness (%)[1]	98.9 (96.7)	99.9 (99.5)	99.9 (99.3)	100.0 (100.0)
Refinement				
R- no σ cutoff (%)	–	11.29	12.22	11.47
R_{free} (%)	–	13.58	15.54	13.08
R.m.s.				
Bond lengths (Å)	–	0.013	0.020	0.015
Angle distance (Å)	–	0.029	0.028	0.030
Average B				
Protein (Å^2)	–	13.5	12.7	9.8
Ligand (Å^2)	–	18.1	17.0	28.1
Atoms				
Protein	–	2764	2763	2828
Inhibitor	–	20	30	–
Other ligand[2]	–	8	7	58
Water sites	–	422	450	466
Disordered side chains	–	19	20	34
S.u. of main chain atoms (Å)[3]	–	0.032	0.037	0.016
PDB accession code		1GA1	1GA4	1GA6

[1]Numbers in parentheses refer to values for the highest-resolution shell.
[2]There is one Ca^{2+} ion present in all models; one Cl$^-$ ion in model B; one glycerol molecule in models B and C; and four glycerol molecules, four acetate ions, and a tyrosine (possibly from the inhibitor, but bound away from the substrate-binding site) in model D.
[3]Average standard uncertainty of atomic positions in the main chain from the inversion of the least-squares matrix. Approximately 92% of the main chain torsion angles are in the most favored region of the Ramachandran plot, with the rest in the additional allowed region.

letters

a substrate peptide bond (or an aldehyde inhibitor), the pK_a value would decrease dramatically and allow Glu 80 to abstract the proton of the –OH group. This glutamic acid is in a stereo-chemically equivalent position to His 64 of subtilisin (Fig. 4*c*) and, by inference, should play the same role as a general base. Glu 80, as described above, is hydrogen bonded to Asp 84, which helps to hold the Glu carboxyl group in the appropriate position to function as the base. Following proton transfer from Ser 287-OH to Glu 80, the proton shared by Glu 80 and Asp 84 would associate more strongly with the latter. The net result of these proton movements would be a strongly nucleophilic Ser 287 oxygen, accompanying bond formation to the carbonyl carbon of the scissile bond.

Simultaneously, the oxygen atom of the peptide or aldehyde carbonyl group would acquire an increased negative charge. Based on the positioning of Asp 170 equivalent to that of Asn 155 in subtilisin, it is reasonable to speculate that a protonated Asp 170 could help stabilize the negative charge by partial donation of a proton to the electronegative oxygen atom. In the case of the aldehyde inhibitor, full transfer of the proton occurs to yield a stable intermediate. More experiments are necessary to verify the enzymatic mechanism for this new family of pro-teinases.

Methods

Crystallization. All the procedures have been described[24]. Protein was cloned and overexpressed in *Escherichia coli*[2]. All crystals were grown from a solution containing a mixture of PSCP with the inhibitor iodotyrostatin (Fig. 3*a*). Crystals A and B (Table 1) were grown at pH 7.5. The Br⁻ derivative (crystal A) was prepared by soaking a crystal for 30 s in the solution containing 1 M sodium bromide. Crystals C and D, grown at pH 3.5, were soaked before use in their respective mother liquors at pH 4.0 for crystal C and pH 5.2 for crystal D. Completely unambiguous density corresponding to the inhibitor bound covalently to Ser 287 could be traced in crystal C (Fig. 3*c*), although the occupancy of the inhibitor was only 0.5. All atoms corresponding to the inhibitor were covered by electron density, although the chemical nature of the inhibitor was not that of the expected iodotyrostatin[25] (Fig. 3*a*), but rather that of a peptide with leucine missing (here called pseudo iodotyrostatin) and corresponding to the sequence isovaleryl-iodoPhe-tyrosinal (Fig. 3*b*). We have established by 1D and 2D NMR, as well as by electrospray mass spectroscopy, that iodotyrostatin was the dominant component of the inhibitor used for preparing PSCP complexes, although minor components were present in the inhibitor sample (data not shown). We assume that pseudo iodotyrostatin must bind to PSCP with much higher affinity than iodotyrostatin and, therefore, it was the only form of the inhibitor that could be traced in crystal C. Only fragments of noncovalently bound inhibitor were seen in other crystals.

Data collection, structure solution and refinement. All X-ray data (Table 1) were collected at 100 K on beamline X9B, NSLS, Brookhaven National Laboratory, with the ADSC Quantum4 CCD detector. Reflections were processed using the HKL2000 suite[26]. Solution of the structure was described[24]. The single wavelength data set collected at the peak of the bromine absorption edge (crystal A) was used exclusively for initial phasing and model building of PSCP. The SHELXD[27] run against the Bijvoet differences identified a number of bromide sites, from which the nine strongest were selected and input to SHARP[28]. The phases were extended to the full resolution of the data collected on crystal B (1.4 Å) by density modification with DM[29] and submitted to automatic map interpretation and model building by wARP[30]. The initial model of 363 out of 372 peptides with the majority of correct side chains and several hundred of waters was constructed automatically, with minimal user intervention, and gave an R factor of 19.9% and R_{free} of 22.6%. The remaining peptides and missing side chains were introduced manually using O[31]. The atomic model of PSCP was refined against three data sets, recorded from crystals B, C and D. All three structures were refined according to the same protocol with SHELXL[32] against F-squared in the conjugate gradient (CGLS) mode. The default restraints were used for geometrical[33] and displacement parameters.

The models were refined first isotropically to convergence and then anisotropically. In all cases, the introduction of anisotropic displacement parameters was validated by the drop in both R and R_{free}. Hydrogen atoms were introduced as rigidly 'riding' on their parent atoms, except for side chains in double conformations. Water oxygen atoms were refined with unit occupancies, although some of the sites were probably only partially occupied. When the process reached convergence at the end of refinement, a round of blocked full-matrix least-squares refinement was performed using all reflections, including those used for R_{free}, to obtain the most accurate model possible and to properly estimate the standard uncertainties of all individual refined parameters from the inversion of the least-squares matrix. The refinement parameters are presented in Table 1.

Coordinates. The coordinates of models B, C, and D have been deposited in the Protein Data Bank (1GA1, 1GA4 and 1GA6, respectively).

1. Oda, K., Sugitani, M., Fukuhara, K. & Murao, S. *Biochim. Biophys. Acta* **923**, 463–469 (1987).
2. Oda, K., Takahashi, T., Tokuda, Y., Shibano, Y. & Takahashi, S. *J. Biol. Chem.* **269**, 26518–26524 (1994).
3. Ito, M., Narutaki, S., Uchida, K. & Oda, K. *J. Biochem. (Tokyo)*, **125**, 210–216 (1999).
4. Oyama, H., Abe, S., Ushiyama, S., Takahashi, S. & Oda, K. *J. Biol. Chem.* **274**, 27815–27822 (1999).
5. Davies, D.R. *Annu. Rev. Biophys. Biophys. Chem.* **19**, 189–215 (1990).
6. Barrett, A.J., Rawlings, N.D. & Woessner, J.F. *Handbook of proteolytic enzymes* (Academic Press, London; 1998).
7. Murao, S. *et al. J. Biol. Chem.* **268**, 349–355 (1993).
8. Shibata, M., Dunn, B.M. & Oda, K. *J. Biochem. (Tokyo)* **124**, 642–647 (1998).
9. Sleat, D.E. *et al. Science* **277**, 1802–1805 (1997).
10. Rawlings, N.D. & Barrett, A.J. *Biochim. Biophys. Acta* **1429**, 496–500 (1999).
11. Lin, L., Sohar, I., Lackland, H. & Lobel, P. *J. Biol. Chem.* **276**, 2249–2255 (2001).
12. Kwon, H.K., Kim, H. & Ahn, T.I. *Korean J. Biol. Sci.* **3**, 221–228 (1999).
13. Wright, C.S., Alden, R.A. & Kraut, J. *Nature* **221**, 235–242 (1969).
14. Holm, L. & Sander, C. *J. Mol. Biol.* **233**, 123–138 (1993).
15. Kuhn, P. *et al. Biochemistry* **37**, 13446–13452 (1998).
16. Robertus, J.D., Kraut, J., Alden, R.A. & Birktoft, J.J. *Biochemistry* **11**, 4293–4303 (1972).
17. Miller, M., Rao, J.K.M., Wlodawer, A. & Gribskov, M.R. *FEBS Lett.* **328**, 275–279 (1993).
18. Dodson, G. & Wlodawer, A. *Trends Biochem. Sci.* **23**, 347–352 (1998).
19. Delbaere, L.T. & Brayer, G.D. *J. Mol. Biol.* **183**, 89–103 (1985).
20. Bullock, T.L., Breddam, K. & Remington, S.J. *J. Mol. Biol.* **255**, 714–725 (1996).
21. Schechter, I. & Berger, A. *Biochem. Biophys. Res. Commun.* **27**, 157–162 (1967).
22. Bode, W., Papamokos, E. & Musil, D. *Eur. J. Biochem.* **166**, 673–692 (1987).
23. Oda, K., Nakatani, H. & Dunn, B.M. *Biochim. Biophys. Acta* **1120**, 208–214 (1992).
24. Dauter, Z., Li, M. & Wlodawer, A. *Acta Crystallogr. D* **57**, 239–249 (2001).
25. Oda, K., Fukuda, Y., Murao, S., Uchida, K. & Kainosho, M. *Agric. Biol. Chem.* **53**, 405–415 (1989).
26. Otwinowski, Z. & Minor, W. *Methods Enzymol.* **276**, 307–326 (1997).
27. Sheldrick, G.M. In *Direct methods for solving macromolecular structures.* (ed. Fortier, S.) 401–411 (Kluwer Academic Publishers, Dordrecht; 1998).
28. de la Fortelle, E. & Bricogne, G. *Methods Enzymol.* **276**, 472–494 (1997).
29. Cowtan, K.D. & Main, P. *Acta Crystallogr. D* **52**, 43–48 (1996).
30. Perrakis, A., Morris, R. & Lamzin, V.S. *Nature Struct. Biol.* **6**, 458–463 (1999).
31. Jones, T.A. & Kjeldgaard, M. *Methods Enzymol.* **277**, 173–208 (1997).
32. Sheldrick, G.M. & Schneider, T.R. *Methods Enzymol.* **277**, 319–343 (1997).
33. Engh, R. & Huber, R. *Acta Crystallogr. A* **47**, 392–400 (1991).
34. Kraulis, P.J. *J. Appl. Crystallogr.* **24**, 946–950 (1991).
35. Carson, M. *J. Appl. Crystallogr.* **24**, 958–961 (1991).